

HETEROCYCLES, Vol. 90, No. 1, 2015, pp. 515 - 528. © 2015 The Japan Institute of Heterocyclic Chemistry
Received, 28th June, 2014, Accepted, 29th July, 2014, Published online, 7th August, 2014
DOI: 10.3987/COM-14-S(K)51

A NEW CLASS OF STRUCTURALLY SIMPLE AND HIGHLY EMISSIVE FLUOROPHORES WITH A PYRIDINE–ACETYLENE–PHENOL CONJUGATE

Yuki Ohishi, Hajime Abe,* and Masahiko Inouye*

Graduate School of Pharmaceutical Sciences, University of Toyama, Sugitani 2630, Toyama 930-0194, Japan. E-mail: abeh@pha.u-toyama.ac.jp

Abstract – A model compound for pyridine–acetylene–phenol conjugates was prepared, and its hydrogen-bonding and spectroscopic properties were studied. Pyridine and phenol moieties worked as a hydrogen-bonding acceptor and a donor, respectively, so that the conjugate model efficiently bound to MeOH. The absorption and fluorescence spectra showed remarkable additive effects against acid and base, illustrating the application of the conjugates to recognition-sensitive fluorophores.

Dedicated to Professor Isao Kuwajima on the occasion of his 77th birthday

INTRODUCTION

Poly- and oligo(aryleneethynylene)s (PAEs and OAEs) are classes of π -conjugated compounds in which aromatic rings are linked with acetylene bonds.¹ Optical properties of PAEs and OAEs have attracted chemists, and various kinds of PAEs and OAEs with functional groups have been developed so far as optical materials. In general, their optical properties are largely influenced by conformational freedom and electronic characteristics of them. Foldable PAEs and OAEs have been studied also in the field of supramolecular chemistry.² Our group has developed oligo- and poly(2,6-pyridyleneethynylene)s **1** as synthetic host molecules, which consisted of pyridine rings linked at their 2,6-positions with acetylene bonds (Figure 1).³ These host molecules can associate with saccharide guests to form helical complexes by multipoint hydrogen-bonding between pyridine nitrogen atoms and saccharide hydroxy groups. In relation to the polypyridine skeletons, we found that host molecules involving pyridine–acetylene–1*H*-4-pyridone moieties are also effective for saccharide recognition.⁴ The pyridine

nitrogen atoms and the 1*H*-4-pyridone N–H groups played roles of a hydrogen-bonding acceptor and a donor, respectively, so that the hosts could bind to a hydroxy group in a push-pull fashion as N⋯HO⋯HN (Figure 2a). The acetylene bond was essential to spatially separate the acceptors and donors for inhibition of their self-interaction. This success let us go on the investigation of a series of combinations of pyridine and other hydrogen-bonding donor moieties.

During the course of this study, we expected that the conjugates of pyridine–acetylene–phenol would interact with a hydroxy group in a push-pull fashion as N⋯HO⋯HO (Figure 2b). However, despite its simple appearance, a little is known for the skeletons in terms of the chemical and optical characteristics.⁵⁻⁷ Thus, we first synthesized the conjugate model **2** in order to develop a new host architecture (Figure 3). Here we report the hydrogen-bonding ability of the model **2** as well as its highly emissive properties responsive to acid/base circumstances.

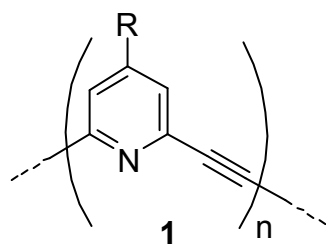


Figure 1. Oligo- and poly(2,6-pyridyleneethynylene)s **1**

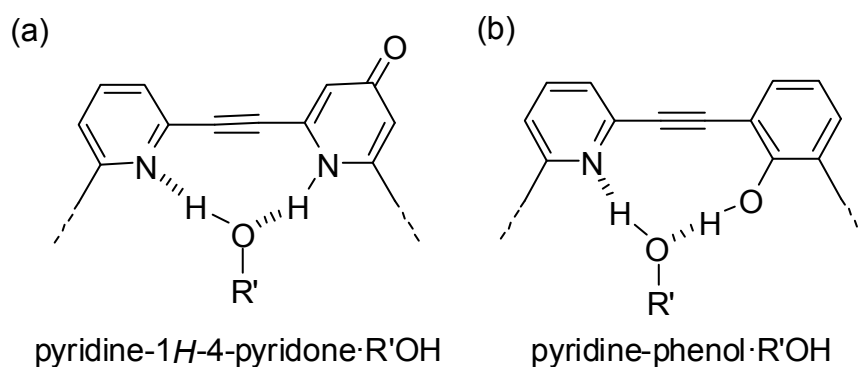


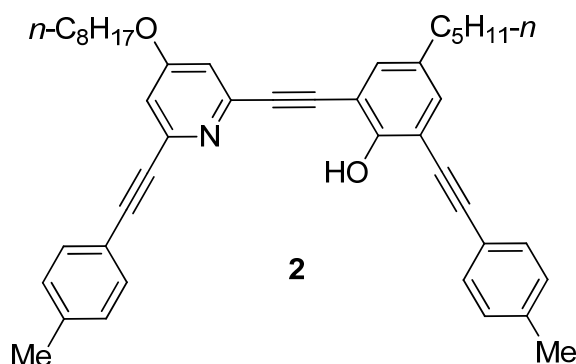
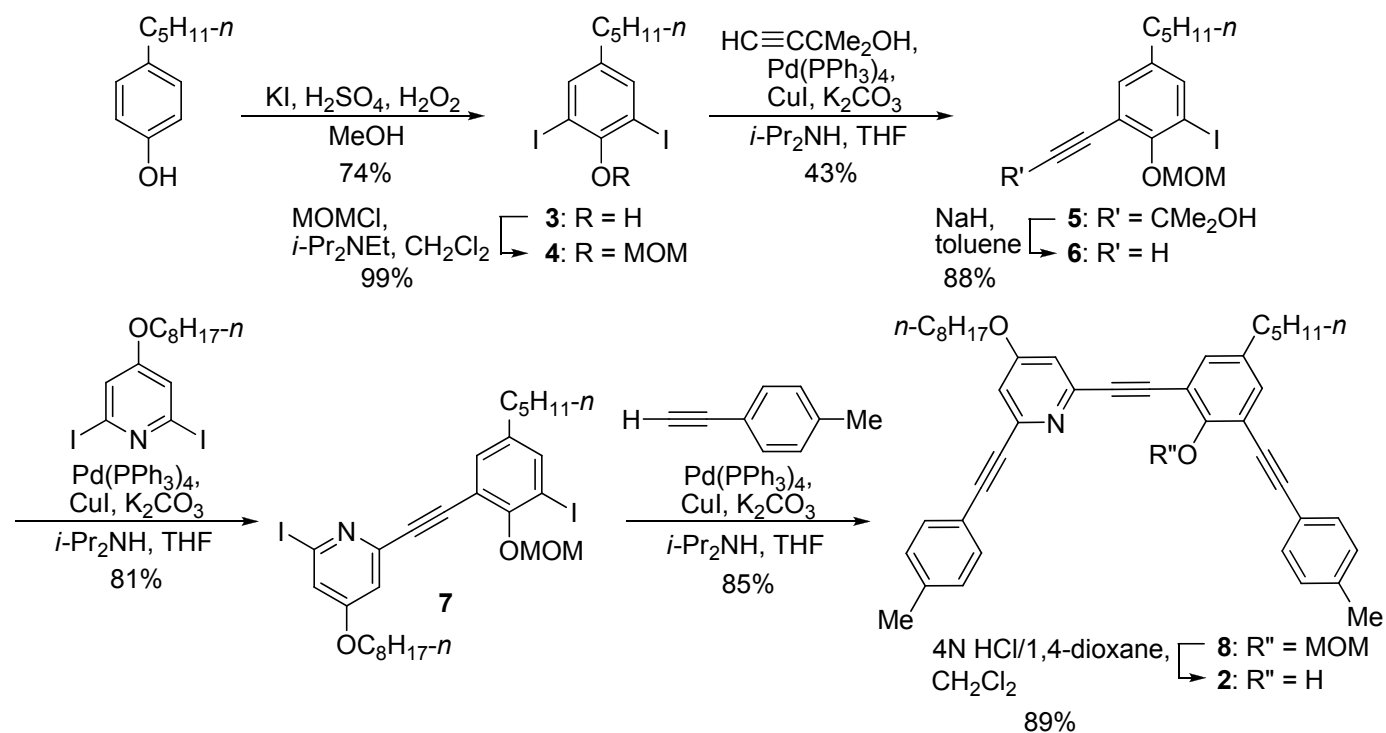
Figure 2. Schematic diagrams of the hydrogen bonds of (a) pyridine–acetylene–1*H*-4-pyridone and (b) pyridine–acetylene–phenol modules with a guest alcohol in a push-pull fashion

RESULTS AND DISCUSSION

Preparation of Pyridine–Acetylene–Phenol Model **2**.

The model **2** was prepared as shown in Scheme 1. Oxidative iodization of commercially available 4-pentylphenol gave 2,6-diiodo-4-pentylphenol (**3**), and the free phenol was protected with a MOM group

to yield **4**. This MOM protection prevents forthcoming acetylene-substituted intermediates from cyclizing to undesirable benzofurans at any palladium-catalyzed steps. Sonogashira reaction of diiodide **4** with 2-methyl-3-butyn-2-ol gave monosubstituted product **5** in a moderate yield, and it was converted to monoyne **6** by liberation of acetone. Monoyne **6** was subjected to Sonogashira reaction with an excess amount of 2,6-diiodo-4-(octyloxy)pyridine⁸ to yield diiodide **7**, which was further coupled with two equivalence of 4-ethynyltoluene to afford **8**. Finally, deprotection of the MOM group with HCl (4N in 1,4-dioxane) furnished the targeted compound **2**.

Figure 3. Pyridine–acetylene–phenol model **2**Scheme 1. Preparation of **2**

Interaction of the Model 2 with MeOH.

To confirm the skeleton being able to interact with hydroxy groups in a push-pull fashion as shown in Figure 2b, the association of **2** with MeOH was studied by ^1H NMR analyses. Figure 4 shows the change of ^1H NMR spectrum of **2** around the aromatic region during the titration with MeOH in CDCl_3 .⁹ The proton signals on the pyridine ring in **2** were observed to shift upfield by the addition of MeOH. This finding can be rationalized by considering the possible conformations of **2**. When **2** forms N-shape conformation, the pyridine protons are much suffered from the electric field effect of the oxygen because the distance between H^a and the hydroxy group is decreased (Figure 5a). The association of **2** with MeOH stabilizes the U-shape conformation that weakens the electric field effect, so that the signal of H^a shifted upfield (Figure 5b). Binding constant $K_{2\text{-MeOH}}$ between **2** and MeOH was estimated to be $1.2 \times 10^1 \text{ M}^{-1}$ by using an iterative least-squares curve-fitting analysis (Figure S3).¹⁰ As the control experiment, the binding was also examined for the simple pyridine derivative **9**⁸ that cannot form hydrogen bonds in a push-pull fashion owing to the lack of a phenol moiety (Figure 6). The binding constant $K_{9\text{-MeOH}}$ between **9** and MeOH was estimated to be $3.7 \times 10^{-1} \text{ M}^{-1}$ by the ^1H NMR titration (Figure S4),¹⁰ and this value was apparently ca. 30 times as small as that of $K_{2\text{-MeOH}}$, demonstrating the importance of the push-pull hydrogen bonds.

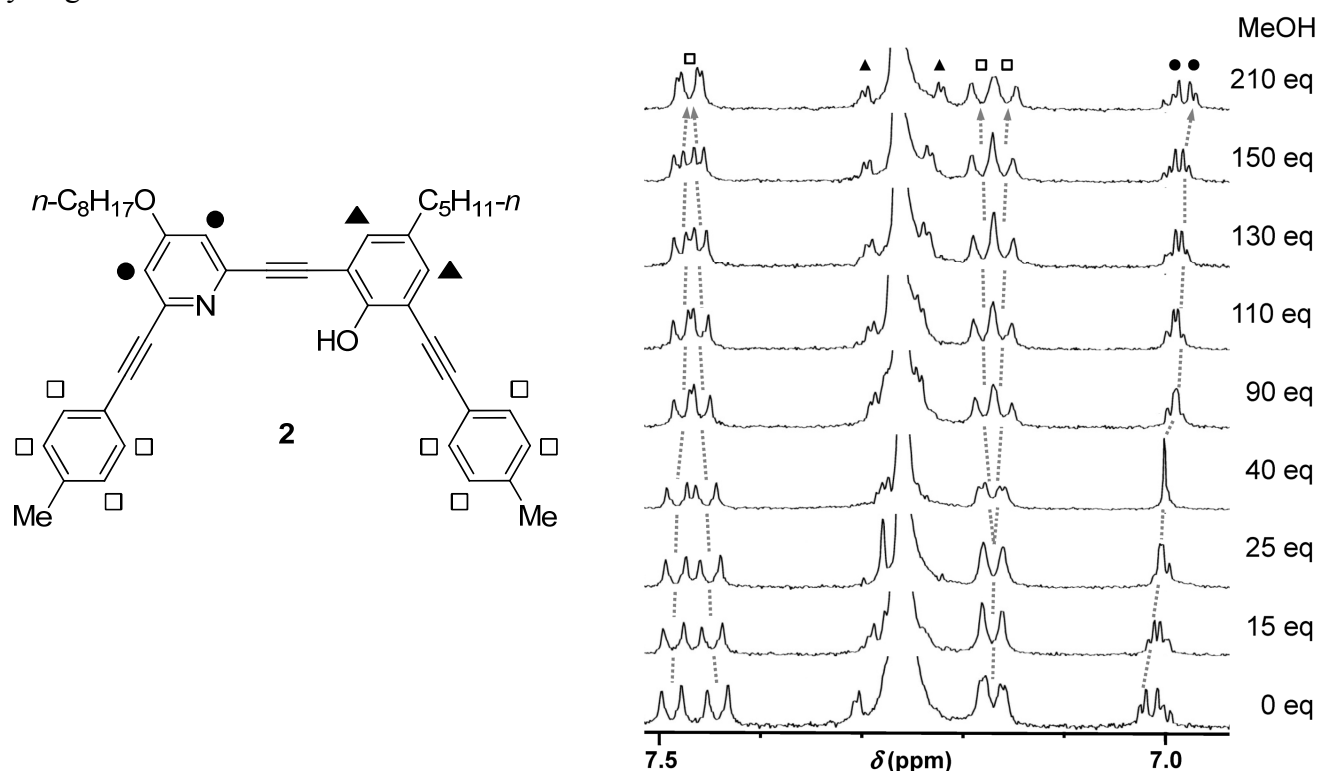


Figure 4. Change of ^1H NMR shifts of **2** during titration with MeOH. Signals shown were assigned to the aromatic protons at pyridine (filled circle), phenol (filled triangle), and tolyl moieties (open square). Conditions; 300 MHz, $[\mathbf{2}] = 7.5 \times 10^{-4} \text{ M}$, $[\text{MeOH}] = 0$ to $1.6 \times 10^{-1} \text{ M}$, CDCl_3 , 23°C .

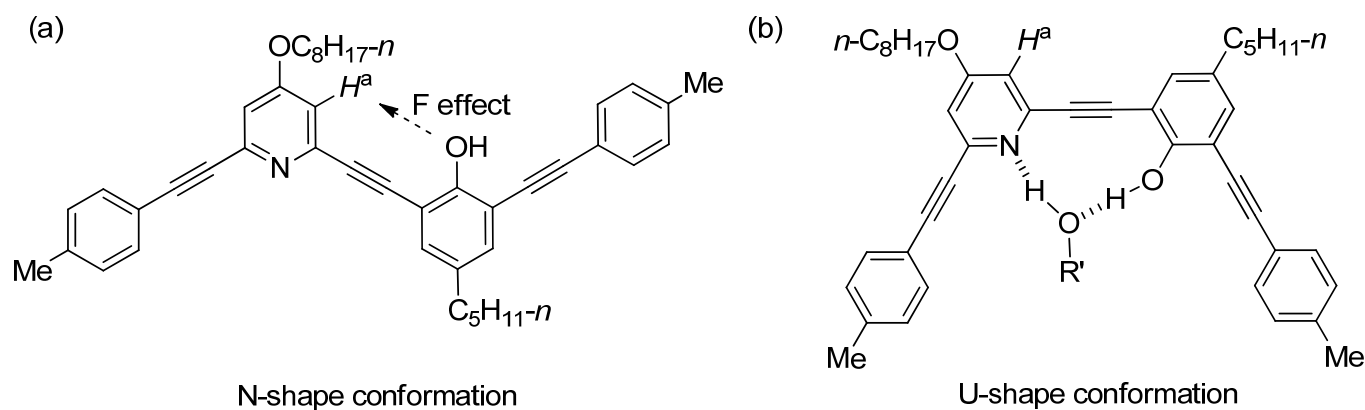


Figure 5. Conformations of **2**. (a) N-shape conformation. (b) U-shape conformation.

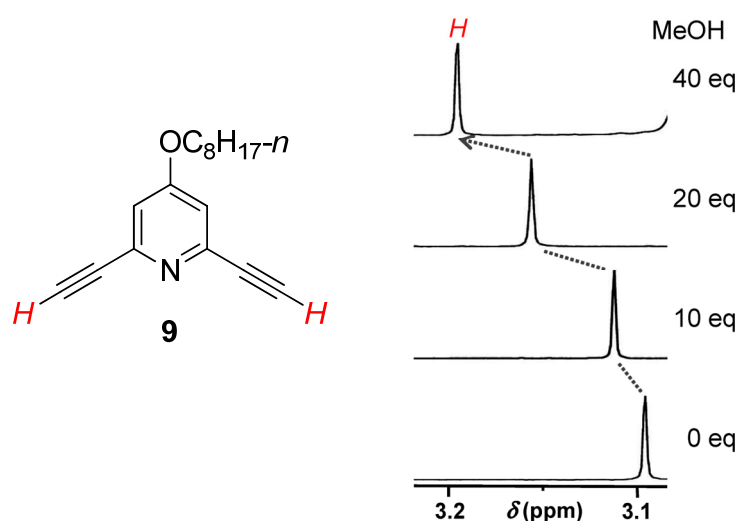


Figure 6. Change of ^1H NMR spectrum of **9** during the titration with MeOH. Signals shown were assigned to the alkyne C-H protons. Conditions; 400 MHz, $[\mathbf{9}] = 3.8 \times 10^{-2}$ M, $[\text{MeOH}] = 0$ to 1.7 M, CDCl_3 , 23 $^\circ\text{C}$.

Optical Properties of the Model **2** and MOM-Protected Precursor **8**.

We studied the optical properties of the model **2** and its MOM-protected precursor **8**. UV-vis and fluorescence emission spectra of **2** and **8** were measured in 1,2-dichloroethane (DCE) solutions (Figure 7). The UV spectrum of **2** showed absorptive bands at $\lambda_{\text{max}} = 281, 291$ nm with small shoulder around 350 nm, while that of **8** at $\lambda_{\text{max}} = 292$ nm (Figure 7, solid lines). The shapes of the fluorescence emission spectra were similar between **2** and **8** (Figure 7, dashed lines), while their fluorescence quantum yields (Φ_f) were substantially different in degassed DCE.¹¹ The Φ_f value of **8** was determined to be 0.98, indicating that the absorbed photons on **8** are almost emitted as fluorescence. Indeed, we have reported that the introduction of alkyne groups into aromatic fluorophores induced a dramatic increase of fluorescence efficiencies compared with the parent fluorophores.¹² Although the deprotected **2** also revealed the substantially large Φ_f value of 0.44, the highly emissive nature of **8** is outstanding. This is

probably because the axial rotation around the acetylene bonds were restricted by the steric hindrance of the MOM group in **8**, so that the nonradiative deactivation decreased resembling the GFP emissive core (Figure 8).¹³

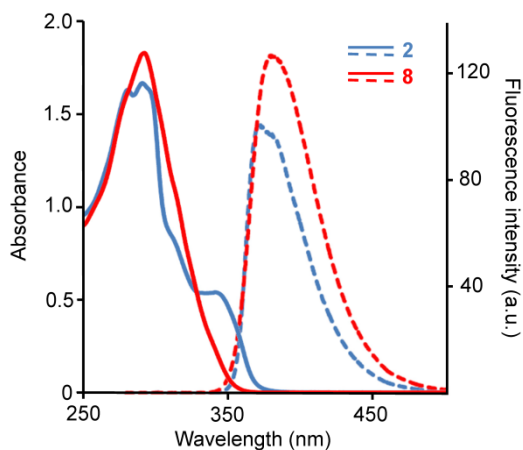


Figure 7. UV-vis (solid lines) and fluorescence emission spectra (dashed lines) of **2** (blue lines) and **8** (red lines). Conditions: [**2**] or [**8**] = 2.5×10^{-5} M, DCE, 25 °C, λ_{ex} = 300 nm, path length = 10 mm.

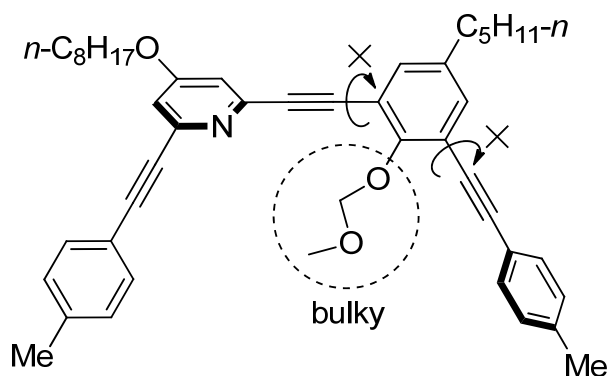


Figure 8. Restriction of axial rotation in **8**

Acid/Base-Responsive Absorption and Fluorescence of the Model **2**.

The model **2** was expected to show acid/base-responsive absorption and fluorescence because the pyridine-phenol combination formally could be a zwitterionic structure. To study the effects of acid, UV-vis spectrum of **2** (1.0×10^{-5} M) was measured in DCE at the presence of trifluoroacetic acid (TFA). The absorptive band around 342 nm was enhanced with red shift and that 291 nm was weakened, according to the addition of TFA up to 2.0×10^{-3} M (Figure 9a). The existence of an isosbestic point at 313 nm indicates the participation of only two kinds of absorptive species, probably **2** and its protonated **10** (Figure 10). The similar acid-induced changes were seen in the case of previously reported 4-dimethylaminopyridine-type polymers.^{3b} The red shift would be due to lowering of the energy level of LUMO caused by the protonation. Figure 9b shows the change of fluorescence spectra during the same

titration with TFA. The emission around 374 nm was quenched, while a very weak band appeared around 456 nm, according to the addition of TFA. The emerging faint peak would correspond to the emission from **10**, however, the possible contribution of emissive species such as CT complex and exciplex could have not been excluded, so further study is necessary.

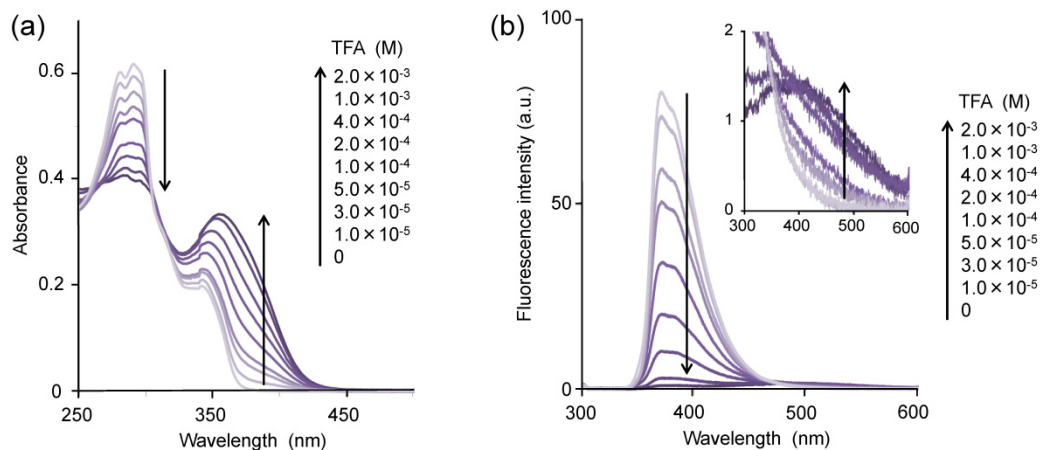


Figure 9. (a) Changes of UV-vis spectrum and (b) fluorescence emission spectrum of **2** during the titration with TFA. Conditions; $[2] = 1.0 \times 10^{-5}$ M, $[TFA] = 0$ to 2.0×10^{-3} M, DCE, 25°C , $\lambda_{\text{ex}} = 300$ nm, path length = 10 mm.

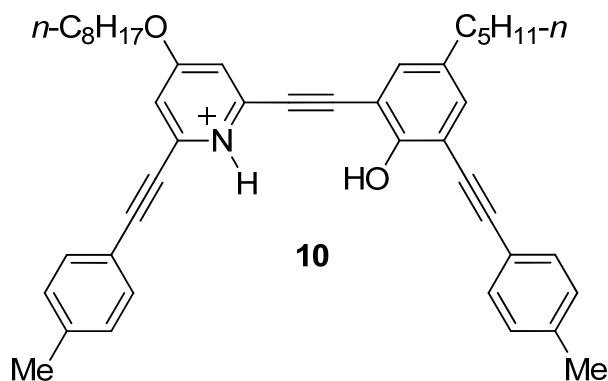


Figure 10. Protonated **10**

The additive effect of base was also studied on the optical properties of **2**. The UV-vis spectrum of **2** (1.0×10^{-5} M) in DCE was measured during the titration with *n*-Bu₄NOH up to 1.0×10^{-3} M. The two absorptive bands around 342 and 291 nm were weakened, and a new band appeared and increased around 446 nm by the addition (Figure 11a). The color of the solution of **2** changed from colorless to yellow as progressing the addition (Figure 11b). The absorbances at 304 and 361 nm were roughly constant during

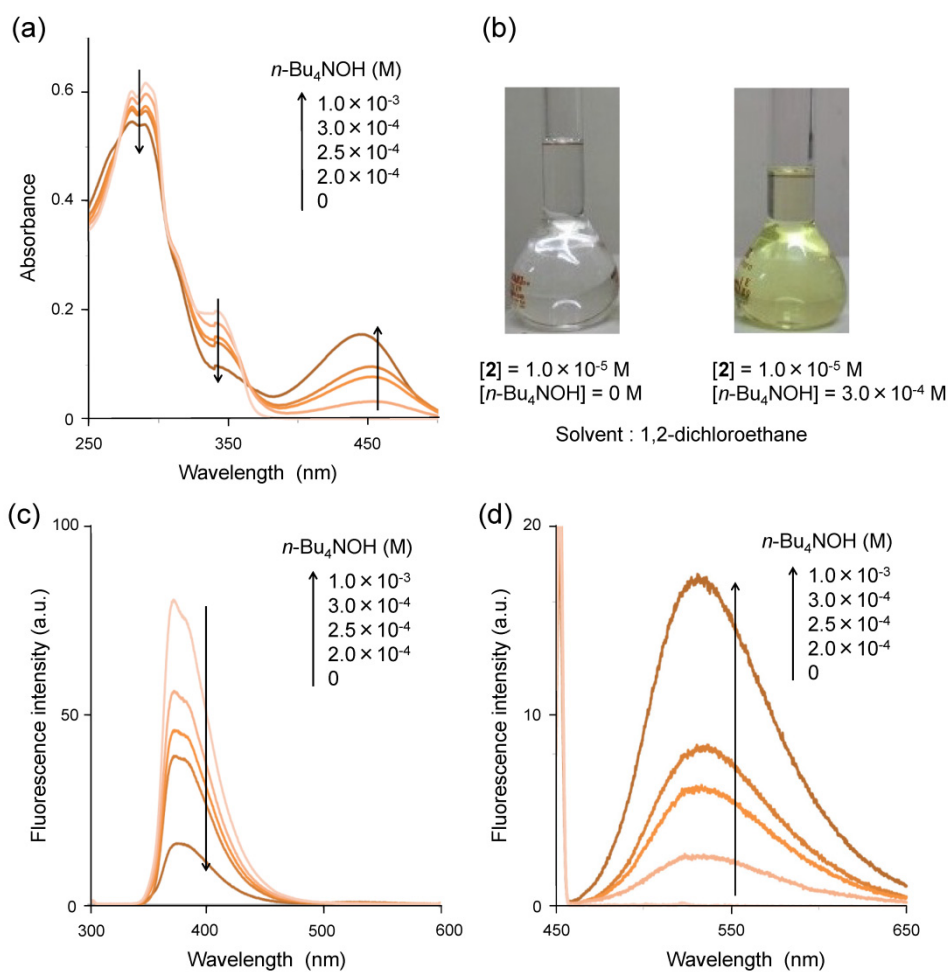


Figure 11. (a) Change of UV-vis spectrum of **2** by the addition of *n*-Bu₄NOH. (b) DCE solutions of **2** before and after the addition of *n*-Bu₄NOH. (c), (d) Change of fluorescence emission spectrum of **2** by the addition of *n*-Bu₄NOH, when **2** was excited at (c) 300 nm and (d) 450 nm. Conditions; [**2**] = 1.0×10^{-5} M, [*n*-Bu₄NOH] = 0 to 1.0×10^{-3} M, DCE, 25 °C, path length = 10 mm.

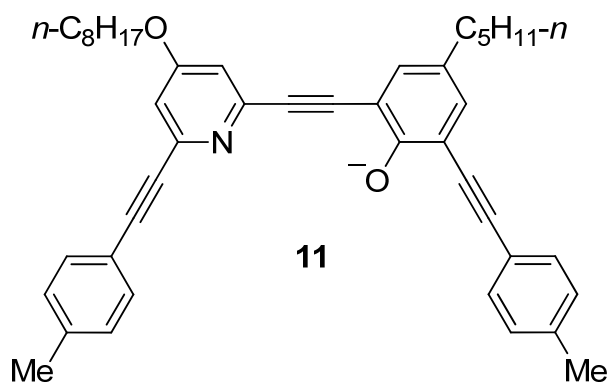


Figure 12. Deprotonated **11**

the titration, so that mainly two kinds of absorptive species are likely to exist, probably **2** and its deprotonated **11**. (Figure 12). The appearance of the absorptive band at the long wavelength could be due to the raised energy levels of the n and π orbitals caused by the deprotonation. In the case of the fluorescence spectrum, the emission around 374 nm was quenched when **2** was excited at 300 nm. On the other hand, a new emission around 535 nm appeared and increased upon excitation at 450 nm that is the absorption maximum of the deprotonated **11** (Figures 11c and 11d).

CONCLUSION

We have studied a new architecture, pyridine–acetylene–phenol conjugates as a molecular recognition motif. The pyridine and phenol worked as a hydrogen-bonding acceptor and a donor, respectively, so that the conjugate model **2** bound to MeOH by hydrogen-bonding in a push-pull fashion. Optical properties and acid/base additive effects were investigated on the basis of absorption and fluorescence emission analyses. Both the spectra clearly changed by the addition of TFA and *n*-Bu₄NOH, demonstrating the conjugates being applicable to recognition-sensitive fluorophores. Based on this finding, we are planning to investigate the longer oligo(pyridine–acetylene–phenol)s, in which pyridine and phenol units are linked alternately at their 2,6-positions with acetylene bonds. Such oligomers are expected as an efficient synthetic signaling receptor for oligosaccharide recognition.

ACKNOWLEDGEMENTS

This work was supported by a JSPS KAKENHI Grant Number 28·9859.

EXPERIMENTAL

General. ¹H and ¹³C NMR spectra were recorded on a Varian GEMINI300 NMR spectrometer by using tetramethylsilane (TMS) as an internal reference. ESI–HRMS analyses were carried out on a JEOL JMS–T100LC mass spectrometer. IR, UV-vis, and fluorescence spectra were obtained by JASCO FT/IR–460plus, V–5601, and FP–6500 spectrometers, respectively. Melting points were determined with a Yanako MP–500D melting point apparatus and not corrected. THF was freshly distilled from sodium benzophenone ketyl before use. DCE of anhydrous grade was used for the spectroscopic analyses. 2,6-Diiodo-4-(octyloxy)pyridine and pyridine derivative **9** were prepared according to the procedures we reported previously.⁸

2,6-Diiodo-4-pentylphenol (3). To a solution of 4-pentylphenol (17.4 g, 106 mmol) in MeOH (580 mL) were slowly added H₂SO₄ (18.8 mL), potassium iodide (38.8 g, 232 mmol), and hydrogen peroxide (30% in water, 48 mL) at 0 °C. The reaction mixture was stirred for 17 h at room temperature. The resulting

mixture was diluted with water (300 mL) and extracted with CH₂Cl₂ (400 mL × 3). The combined organic layer was washed with aqueous NaHSO₃ (0.1 M, 1 L) and water (500 mL) subsequently, dried over Na₂SO₄, and then concentrated by a rotary evaporator. The resulting viscous oil was subjected to silica gel column chromatography (eluent; hexane) to afford **3** (32.6 g, 74%) as a colorless solid: mp 47–48 °C; ¹H NMR (CDCl₃, 300 MHz) δ 7.25 (s, 2 H), 5.57 (s, 1 H), 2.44 (t, *J* = 7.8 Hz, 2 H), 1.54 (m, 2 H), 1.36–1.22 (m, 4 H), 0.89 (t, *J* = 6.9 Hz, 3 H); ¹³C NMR (CDCl₃, 75 MHz) δ 151.2, 138.9, 138.8, 82.0, 34.0, 31.3, 31.1, 22.5, 14.1; IR (neat) ν_{\max} 3443, 2964, 2950, 2915, 2852, 1746, 1542 cm⁻¹; HRMS (ESI–TOF) calcd for C₁₁H₁₄I₂NaO (M + Na⁺): 438.9032; found: 438.9047.

1,3-Diiodo-2-(methoxymethoxy)-5-pentylbenzene (4). To a stirred solution of **3** (11.3 g, 27.1 mmol) in CH₂Cl₂ (108 mL) was added chloromethyl methyl ether (10.9 g, 135 mmol) at 0 °C. To the reaction mixture was added *i*-Pr₂NEt (14.0 g, 108 mmol) dropwise during 30 min at 0 °C, and after that it was additionally stirred for 30 min at 0 °C. The resulting mixture was quenched with saturated aqueous NaHCO₃ (100 mL), and extracted with AcOEt (100 mL × 3). The combined organic layer was washed with brine (100 mL), then dried over Na₂SO₄, and concentrated by a rotary evaporator to yield **4** (12.4 g, 99%) as a colorless oil: ¹H NMR (CDCl₃, 300 MHz) δ 7.59 (s, 2 H), 5.11 (s, 2 H), 3.75 (s, 3 H), 2.47 (t, *J* = 7.8 Hz, 2 H), 1.58–1.53 (m, 2 H), 1.34–1.27 (m, 4 H), 0.90 (t, *J* = 6.9 Hz, 3 H); ¹³C NMR (CDCl₃, 75 MHz) δ 153.8, 142.9, 139.7, 99.9, 91.0, 58.8, 34.2, 31.4, 30.9, 22.5, 14.1; IR (neat) ν_{\max} 2954, 2927, 2856, 1577, 1531 cm⁻¹; HRMS (ESI–TOF) calcd for C₁₃H₁₈I₂NaO₂ (M + Na⁺): 482.9294; found: 482.9290.

1-(3-Hydroxy-3-methyl-1-butynyl)-3-iodo-2-(methoxymethoxy)-5-pentylbenzene (5). To a mixture of **4** (16.5 g, 35.9 mmol), Pd(PPh₃)₄ (1.45 g, 1.26 mmol), K₂CO₃ (19.8 g, 144 mmol), and 2-methyl-3-butyn-2-ol (2.11 g, 25.1 mmol) in *i*-Pr₂NH (140 mL) and THF (140 mL) was added CuI (70.2 mg, 0.359 mmol) at room temperature. The mixture was stirred under reflux for 9 h, and the resulting mixture was diluted with Et₂O (100 mL) and filtered through a Florisil bed. The bed was given a rinse with Et₂O. The combined filtrate was concentrated by a rotary evaporator, and the resulting residue was purified by silica gel column chromatography (eluent; AcOEt/hexane = 1:5) to afford recovered **4** (6.84 g, 41%) and **5** (6.46 g, 43% based on 2-methyl-3-butyn-2-ol) as a yellow oil: ¹H NMR (CDCl₃, 300 MHz) δ 7.56 (d, *J* = 1.8 Hz, 1 H), 7.18 (d, *J* = 1.8 Hz, 1 H), 5.24 (s, 2H), 3.70 (s, 3 H), 2.47 (t, *J* = 8.1 Hz, 3 H), 1.60–1.39 (m, 8 H), 1.37–1.23 (m, 4 H), 0.89 (t, *J* = 6.9 Hz, 3 H); ¹³C NMR (CDCl₃, 75 MHz) δ 155.3, 140.2, 139.5, 133.6, 116.3, 99.3, 98.6, 91.8, 81.1, 78.2, 65.5, 58.5, 34.5, 31.4, 31.3, 30.9, 22.5, 14.1; IR (neat) ν_{\max} 3418, 2956, 2929, 2857, 1590, 1547 cm⁻¹; HRMS (ESI–TOF) calcd for C₁₈H₂₅INaO₃ (M + Na⁺): 439.0746; found: 439.0732.

1-(1-Ethynyl)-3-iodo-2-(methoxymethoxy)-5-pentylbenzene (6). To a toluene (30 mL) suspension of NaH (7.6 mg, 0.19 mmol; commercial 60% dispersion was washed thoroughly with hexane prior to use) was added **5** (0.198 g, 0.475 mmol) at room temperature. The mixture was stirred under reflux for 30 min and diluted with water (30 mL). The resulting mixture was extracted with AcOEt (30 mL \times 3), and the combined organic layer was washed with water (60 mL) and brine (60 mL), subsequently, then dried over Na₂SO₄, and concentrated by a rotary evaporator. The resulting residue was purified by silica gel column chromatography (eluent; AcOEt/hexane = 1:30) to yield **6** (0.150 g, 88%) as a yellow oil: ¹H NMR (CDCl₃, 300 MHz) δ 7.61 (m, 2 H), 5.26 (s, 2 H), 3.70 (s, 3 H), 3.27 (s, 1 H), 2.49 (d, J = 7.7 Hz, 2 H), 1.59–1.54 (m, 2 H), 1.32–1.27 (m, 4 H), 0.89 (t, J = 7.2 Hz, 3 H); ¹³C NMR (CDCl₃, 75 MHz) δ 155.9, 140.2, 140.1, 134.2, 116.0, 99.5, 91.9, 81.7, 79.8, 58.4, 34.4, 31.3, 30.8, 22.5, 14.0; IR (neat) ν_{\max} 3292, 2955, 2928, 2857, 2107, 1543 cm⁻¹; HRMS (ESI-TOF) calcd for C₁₅H₁₉INaO₂ (M + Na⁺): 381.0327; found: 381.0326.

2-Iodo-6-((3-iodo-2-(methoxymethoxy)-5-pentylphenyl)ethynyl)-4-(octyloxy)pyridine (7). To a mixture of **6** (1.04 g, 2.89 mmol), Pd(PPh₃)₄ (0.167 g, 0.145 mmol), K₂CO₃ (1.60 g, 11.6 mmol), and 2,6-diiodo-4-(octyloxy)pyridine (7.94 g, 17.3 mmol)⁸ in *i*-Pr₂NH (60 mL) and THF (120 mL) was added CuI (28.2 mg, 0.145 mmol) at room temperature. The mixture was stirred under reflux for 12 h. The resulting mixture was diluted with Et₂O (100 mL) and filtered through a Florisil bed. The bed was given a rinse with Et₂O. The combined filtrate was concentrated by a rotary evaporator, and the resulting residue was purified by silica gel column chromatography (eluent; AcOEt/hexane = 1:30) to yield **7** (1.62 g, 81%) as a colorless oil: ¹H NMR (CDCl₃, 300 MHz) δ 7.63 (d, J = 2.1 Hz, 1 H), 7.35 (d, J = 2.4 Hz, 1 H), 7.20 (d, J = 2.4 Hz, 1 H), 6.98 (d, J = 2.4 Hz, 1 H), 5.30 (s, 2 H), 3.98 (t, J = 3.3 Hz, 2 H), 3.72 (s, 3 H), 2.50 (t, J = 7.8 Hz, 2 H), 1.81–1.76 (m, 2 H), 1.56–1.55 (m, 2 H), 1.41–1.29 (m, 14 H), 0.92–0.88 (m, 6 H); ¹³C NMR (CDCl₃, 75 MHz) δ 164.8, 155.8, 144.0, 140.6, 140.4, 134.1, 120.5, 117.9, 115.9, 114.0, 99.8, 91.9, 91.6, 86.2, 68.7, 58.6, 34.5, 31.8, 31.3, 30.8, 29.3, 29.2, 28.9, 28.8, 25.9, 22.7, 22.5, 14.2, 14.1; IR (neat) ν_{\max} 2955, 2928, 2856, 2218, 1575, 1531 cm⁻¹; HRMS (ESI-TOF) calcd for C₂₈H₃₇I₂NNaO₃ (M + Na⁺): 712.0760; found: 712.0733.

2-((2-(Methoxymethoxy)-5-pentyl-3-(*p*-tolylethynyl)phenyl)ethynyl)-4-(octyloxy)-6-(*p*-tolylethynyl)pyridine (8). To a mixture of **7** (1.84 g, 3.28 mmol), K₂CO₃ (1.81 g, 13.1 mmol), and 4-ethynyltoluene (1.14 g, 9.85 mmol) in *i*-Pr₂NH (65 mL) and THF (130 mL) was added Pd(PPh₃)₄ (189 mg, 0.164 mmol) at room temperature, and the mixture was stirred under reflux for 15 h. The resulting mixture was diluted with Et₂O (100 mL), filtered through a Florisil bed. The bed was given a rinse with Et₂O. The combined filtrate was concentrated by a rotary evaporator, and the resulting residue was purified by silica gel

column chromatography (eluent; AcOEt/hexane = 1:30) to yield **8** (1.49 g, 85%) as a colorless oil: ^1H NMR (CDCl_3 , 300 MHz) δ 7.50–7.47 (m, 2 H), 7.43–7.41 (m, 2 H), 7.39–7.33 (m, 2 H), 7.17–7.15 (m, 4 H), 7.00–6.98 (m, 2 H), 5.46 (s, 2 H), 4.03 (t, J = 6.6 Hz, 2 H), 3.72 (s, 3 H), 2.57–2.51 (t, J = 7.8 Hz, 2 H), 2.37 (s, 6 H), 1.83–1.79 (m, 2 H), 1.63–1.58 (m, 2 H), 1.46–1.31 (m, 14 H), 0.93–0.87 (m, 6 H); ^{13}C NMR (CDCl_3 , 75 MHz) δ 165.5, 156.9, 144.9, 144.5, 139.2, 138.5, 138.4, 134.3, 133.9, 131.9, 131.3, 129.0, 120.0, 119.0, 117.6, 116.4, 113.0, 112.9, 99.3, 93.6, 92.2, 89.3, 87.9, 85.5, 85.0, 68.4, 57.8, 34.8, 31.8, 31.3, 30.8, 29.30, 29.25, 28.9, 26.0, 22.7, 22.6, 21.7, 21.6, 14.2, 14.1; IR (neat) ν_{max} 3029, 2953, 2926, 2856, 2218, 1579, 1550 cm^{-1} ; HRMS (ESI–TOF) calcd for $\text{C}_{46}\text{H}_{51}\text{NNaO}_3$ ($\text{M} + \text{Na}^+$): 688.3767; found: 688.3743.

2-((2-Hydroxy-5-pentyl-3-(*p*-tolylethynyl)phenyl)ethynyl)-4-(octyloxy)-6-(*p*-tolylethynyl)pyridine (**2**).

To a solution of **8** (216 mg, 0.325 mmol) in CH_2Cl_2 (21 mL) was added HCl (4N in dioxane, 0.81 mL, 3.2 mmol) at 0 °C. The mixture was stirred for 30 min and then quenched with saturated aqueous NaHCO_3 (20 mL). The resulting mixture was extracted with CH_2Cl_2 (20 mL \times 3), and the combined organic layer was washed with brine (30 mL), dried over Na_2SO_4 , and then concentrated by a rotary evaporator. The resulting residue was purified by silica gel column chromatography (eluent; AcOEt/hexane = 1:10) to yield **2** (180 mg, 89%) as a colorless solid: mp 59–60 °C; ^1H NMR (CDCl_3 , 300 MHz) δ 7.41–7.39 (m, 2 H), 7.37–7.34 (m, 2 H), 7.29–7.24 (m, 2 H), 7.13–7.08 (m, 4 H), 6.98–6.89 (m, 2 H), 3.93 (t, J = 6.3 Hz, 2 H), 2.51–2.46 (t, J = 7.5 Hz, 2 H), 2.34 (s, 3 H), 2.32 (s, 3 H), 1.76–1.69 (m, 2 H), 1.62–1.52 (m, 2 H), 1.38–1.21 (m, 14 H), 0.92–0.86 (m, 6 H); ^{13}C NMR (CDCl_3 , 75 MHz) δ 165.0, 156.2, 144.3, 144.1, 139.0, 138.2, 134.2, 133.4, 132.8, 131.8, 131.3, 128.9, 128.8, 119.7, 118.8, 113.0, 112.5, 110.8, 109.0, 94.9, 93.2, 89.5, 87.6, 84.9, 83.7, 68.4, 34.6, 31.8, 31.3, 30.9, 29.3, 29.2, 28.8, 25.8, 22.7, 22.5, 21.6, 21.5, 14.13, 14.06; IR (neat) ν_{max} 2925, 2855, 2216, 1581, 1549 cm^{-1} ; HRMS (ESI–TOF) calcd for $\text{C}_{44}\text{H}_{47}\text{NNaO}_3$ ($\text{M} + \text{Na}^+$): 644.3504; found: 644.3478.

REFERENCES

1. For recent reviews of OAEs and PAEs: (a) U. H. F. Bunz, *Chem. Rev.*, 2000, **100**, 1605; (b) ‘*Poly(arylene ethynylene)s*’, ed. by C. Weder, Springer-Verlag, Berlin, 2005; (c) U. H. F. Bunz, *Macromol. Rapid Commun.*, 2009, **30**, 772.
2. For reviews of foldable OAEs and PAEs: (a) D. J. Hill, M. J. Mio, R. B. Prince, T. S. Hughes, and J. S. Moore, *Chem. Rev.*, 2001, **101**, 3893; (b) ‘*Foldamers*’, ed. by S. Hecht and I. Huc, Wiley-VCH, Weinheim, 2007.
3. (a) M. Inouye, M. Waki, and H. Abe, *J. Am. Chem. Soc.*, 2004, **126**, 2022; (b) H. Abe, N. Masuda, M. Waki, and M. Inouye, *J. Am. Chem. Soc.*, 2005, **127**, 16189; (c) M. Waki, H. Abe, and M. Inouye,

- Chem. Eur. J.*, 2006, **12**, 7839; (d) M. Waki, H. Abe, and M. Inouye, *Angew. Chem. Int. Ed.*, 2007, **46**, 3059; (e) H. Abe, S. Takashima, T. Yamamoto, and M. Inouye, *Chem. Commun.*, 2009, 2121; (f) S. Takashima, H. Abe, and M. Inouye, *Chem. Commun.*, 2011, **47**, 7455; (g) S. Takashima, T. Yamamoto, H. Abe, and M. Inouye, *Heterocycles*, 2012, **84**, 355; (h) H. Abe, H. Makida, and M. Inouye, *Tetrahedron*, 2012, **68**, 4353; (i) H. Abe, Y. Ohishi, and M. Inouye, *J. Org. Chem.*, 2012, **77**, 5209; (j) H. Abe, K. Okada, H. Makida, and M. Inouye, *Org. Biomol. Chem.*, 2012, **10**, 6930; (k) H. Abe, H. Makida, and M. Inouye, *Heterocycles*, 2012, **86**, 955; (l) F. Kayamori, H. Abe, and M. Inouye, *Eur. J. Org. Chem.*, 2013, **9**, 1677; (m) S. Takashima, H. Abe, and M. Inouye, *Tetrahedron: Asymmetry*, 2013, **24**, 527; (n) H. Abe, D. Suzuki, A. Shimizu, and M. Inouye, *Heterocycles*, 2014, **88**, 547.
4. (a) M. Inouye, K. Takahashi, and H. Nakazumi, *J. Am. Chem. Soc.*, 1999, **121**, 341; (b) H. Abe, Y. Chida, H. Kurokawa, and M. Inouye, *J. Org. Chem.*, 2011, **76**, 3366. See also ref 8.
5. For a pyridine-phenol module as synthetic intermediates: H. Tsuji, G. M. O. Favier, C. Mitui, S. Lee, D. Hashizume, and E. Nakamura, *Chem. Lett.*, 2011, **40**, 576.
6. For a pyridine-phenol module as ligands: (a) A. Khatyr and R. Ziessel, *Org. Lett.*, 2001, **3**, 1857; (b) A. A. Karpov, A. V. Cherkasov, G. K. Fukin, A. S. Shavyrin, L. Luconi, G. Giambastiani, and A. A. Trifonov, *Organometallics*, 2013, **32**, 2379.
7. The combination of pyridine-alkoxybenzene has been studied. See: (a) M. Hirohata, K. Tada, T. Kawai, M. Onoda, and K. Yoshino, *Synth. Met.*, 1997, **85**, 1273; (b) H. Huang, K. Wang, W. Tan, D. An, X. Yang, S. Huang, Q. Zhai, L. Zhou, and Y. Jin, *Angew. Chem. Int. Ed.*, 2004, **43**, 5635; (c) S. Shotwell, P. M. Windschief, M. D. Smith, and U. H. F. Bunz, *Org. Lett.*, 2004, **6**, 4151; (d) Y. Yamaguchi, S. Kobayashi, T. Wakamiya, Y. Matsubara, and Z. Yoshida, *Angew. Chem. Int. Ed.*, 2005, **44**, 7040; (e) R. Pizzoferrato, T. Ziller, A. Micozzi, A. Ricci, C. L. Sterzo, A. Ustione, C. Oliva, and A. Cricenti, *Chem. Phys. Lett.*, 2005, **414**, 234; (f) Y. Yamaguchi, T. Tanaka, S. Kobayashi, T. Wakamiya, Y. Matsubara, and Z. Yoshida, *J. Am. Chem. Soc.*, 2005, **127**, 9332; (g) J. Schappel, K. Schmidt, and E. Klemm, *J. Polym. Sci. A. Polym. Chem.*, 2005, **43**, 3574; (h) X. Zhao, M. R. Pinto, L. M. Hardison, J. Mwaura, J. Müller, H. Jiang, D. Witker, V. D. Kleiman, J. R. Reynolds, and K. S. Schanze, *Macromolecules*, 2006, **39**, 6355; (i) M. G. Lauer, J. W. Leslie, A. Mynar, S. A. Stamper, A. D. Martinez, A. J. Bray, S. Nagassi, K. McDonald, E. Ferraris, A. Muzny, S. Mcavoy, C. P. Miller, K. A. Walters, K. C. Russell, E. Wang, B. Nuez, and C. Parish, *J. Org. Chem.*, 2008, **73**, 474; (j) K. Becker, M. Fritzsche, S. Höger, and J. M. Lupton, *J. Phys. Chem. B.*, 2008, **112**, 4849; (k) Y. Hu, Y. Xiao, H. Huang, D. Yin, X. Xiao, and W. Tan, *Chem. Asian J.*, 2011, **6**, 1500; (l) Q. Ren, C. G. Reedy, E. A. Terrell, J. M. Wieting, R. W. Wagie, J. P. Asplin, L. M. Doyle, S. J. Long, M. T. Everard, J. S. Sauer, C. E. Baumgart, J. S. D'Acchioli, and N. P. Bowling, *J. Org. Chem.*, 2012, **77**, 2571; (m) K. Seehafer, M.

- Bender, and U. H. F. Bunz, *Macromolecules*, 2014, **47**, 922.
8. H. Abe, H. Machiguchi, S. Matumoto, and M. Inouye, *J. Org. Chem.*, 2008, **73**, 4650.
 9. Prior to the titration experiment with MeOH, the concentration dependence of **2** on ^1H NMR chemical shifts in CDCl_3 was studied to know the strength of self-association. As a result, the self-dimerization constant K_{dim} was obtained as $1.9 \times 10^{-1} \text{ M}^{-1}$, indicating that the self-association is negligible at $[\mathbf{2}] = 7.5 \times 10^{-1} \text{ M}$. For details, see Supporting Information.
 10. Because the binding was weak, it was necessary to use an excess amount of MeOH in order to gain a titration curve suitable for a curve-fitting analysis with the proper range of “probability of binding” $[\text{host} \cdot \text{MeOH}]/[\text{host}]_0$. Therefore, the binding constants may be affected by hydrogen-bonding self-association of MeOH and inconstancy of medium effects on host and host·MeOH. Anyway, qualitatively binding of **2** with MeOH will be stronger than that of **9** with MeOH. For references, see. (a) ‘*Binding Constants: The Measurement of Molecular Complex Stability*’, ed. by K. A. Connors, Wiley, New York, 1987; (b) P. Thordarson, *Chem. Soc. Rev.*, 2011, **40**, 1305.
 11. Fluorescence quantum yields (Φ_f) of **2** and **8** were determined by a comparative method using α -naphthylamine in distilled *n*-hexane ($\Phi_f = 0.48$) as a reference. For details, see Supporting Information.
 12. H. Maeda, T. Maeda, K. Mizuno, K. Fujimoto, H. Shimizu, and M. Inouye, *Chem. Eur. J.*, 2006, **12**, 824; H. Shimizu, K. Fujimoto, M. Frusyo, H. Maeda, Y. Nanai, K. Mizuno, and M. Inouye, *J. Org. Chem.*, 2007, **72**, 1530.
 13. D. Mandal, T. Tahara, N. M. Webber, and S. R. Meech, *Chem. Phys. Lett.*, 2002, **358**, 495.